

Variation of N_d and V_{fb} for different compositions of $CdSe_xTe_{1-x}$ thin films by pulse plating technique

V. Saaminathan^{a,*}, K.R. Murali^b

^aCenter for Smart System and Innovation, Faculty of Engineering, Multimedia University, Malaysia

^bECMS division, Center Electrochemical Research Institute, Karaikudi, India

Received 16 November 2005; accepted 16 November 2005

Abstract

$CdSe_xTe_{1-x}$ thin films with $0 < x < 1$ have been pulse electrodeposited on titanium (Ti), nickel (Ni) and stainless-steel (SS) substrates with different duty cycles. The size of the particles could be controlled by the pulse parameters. The deposition was carried out at room temperature for 1 h under potentiostatic mode with $CdSO_4$, SeO_2 , TeO_2 and H_2SO_4 as precursors. As-deposited and annealed films coated on Ti, Ni and SS were characterized by X-ray diffraction technique and SEM, and their electrical properties were studied. The as-deposited films exhibited a cubic structure; those after heat treatment at $500^\circ C$ in air exhibited a hexagonal structure. Variation of donor concentration and the flat band potential for different values of 'x' and duty cycles were studied for $CdSe_xTe_{1-x}$ thin films. The semiconductor parameters for all compositions coated on Ti, Ni and SS were estimated. It showed good agreement with the earlier reports.

© 2005 Elsevier B.V. All rights reserved.

Keywords: Semiconductor; Thin films; Flat band potential; Carrier concentration; Pulse plating

1. Introduction

II–VI semiconductor thin films and their pseudobinaries are very promising materials for various types of semiconductor devices. The pseudobinaries based on CdSe and CdTe are of special mention in this context. Several researchers with respect to their electrical, optical, structural and other properties have extensively studied CdSe and CdTe thin films and bulk [1–3]. The pseudobinary $CdSe_xTe_{1-x}$ with x varying from 0 to 1 is an important class of semiconductor materials. $CdSe_xTe_{1-x}$ ($0 < x < 1$) is a semiconductor whose band gap (E_g) can be varied by varying the composition (x).

These $CdSe_xTe_{1-x}$ materials can be prepared as thin films by electron beam evaporation [4], thermal flash evaporation [5], slurry painting [6,7], physical vapor deposition [8], electrodeposition [9], pulse electrodeposition [10] and three source elemental evaporation [11]. Pulse

electrodeposition has distinct advantage compared to conventional electrodeposition, viz., [12,13] better adhesion, crack-free and hard deposit, fine-grained films with more uniformity and lower porosity, faster plating rates due to increased permissible current densities, less hydrogen uptake and lower impurity content, and more number of parameters can be varied, i.e., ON time, OFF time and current densities. In the present context, $CdSe_xTe_{1-x}$ films were pulse plated from an acidic solution with duty cycles less than 50–3%.

2. Experimental

$CdSe_xTe_{1-x}$ films were deposited by using the conventional three-electrode cell with graphite as anode, conducting substrate like titanium or tin oxide on glass as cathode, and SCE as a reference electrode. The deposition bath consists of an aqueous solution of 0.1 M $CdSO_4$, 10^{-2} – 10^{-3} M SeO_2 and TeO_2 [14,15]. The pH of the solution was adjusted to 2 by adding dilute sulfuric acid. The deposition was carried out at room temperature for 1 h at -750 mV vs. SCE under potentiostatic condition. The

*Corresponding author.

E-mail addresses: saaminathan.viswanathan@mmu.edu.my, saaminathanv@hotmail.com (V. Saaminathan).

duty cycle was varied from 6.25% to 50% for all compositions of $CdSe_xTe_{1-x}$. The thickness of the films was estimated by gravimetric method.

The films were characterized by X-ray diffraction (XRD) using a JOEL model JDX-8030 XRD unit with $CuK\alpha$ radiation. The conductivity of the films was measured using the two-probe technique.

Capacitance voltage measurements were carried out with sodium sulfate as the electrolyte using an EG&G PARC impedance analyzer at different DC bias voltages and at a constant frequency of 10 kHz [16–20]. The results obtained, i.e., type of semiconductor, flat band potential, donor concentration, band bending and depletion layer width for the films deposited on Ti, Ni and SS substrates.

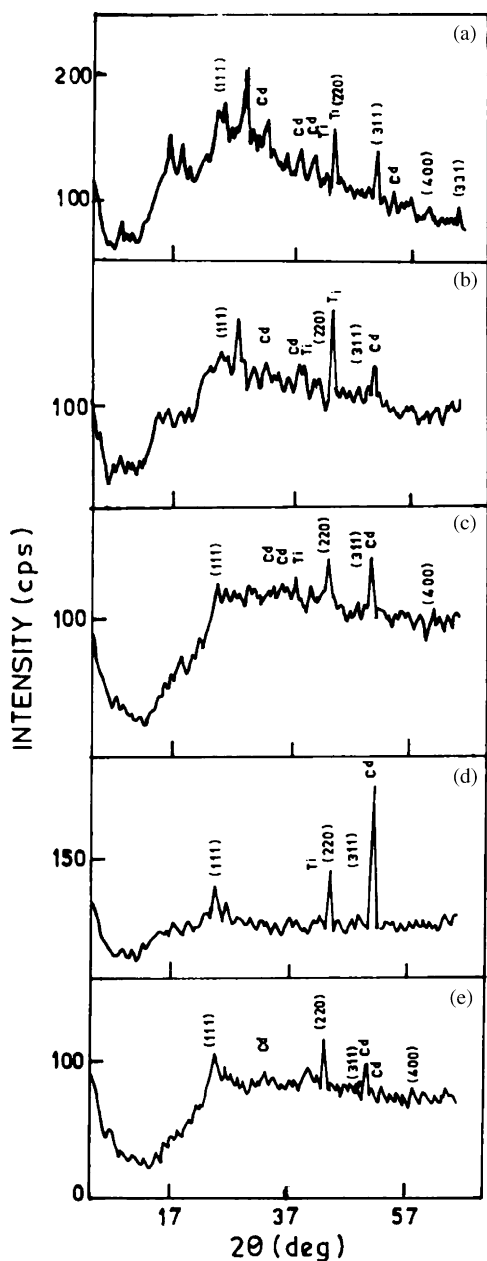


Fig. 1. XRD pattern of pulse plated $CdSeTe_{0.5}Te_{0.5}$ films at different duty cycles on a Ti substrate: (a) 50%, (b) 33%, (c) 15%, (d) 9% and (e) 6.25%.

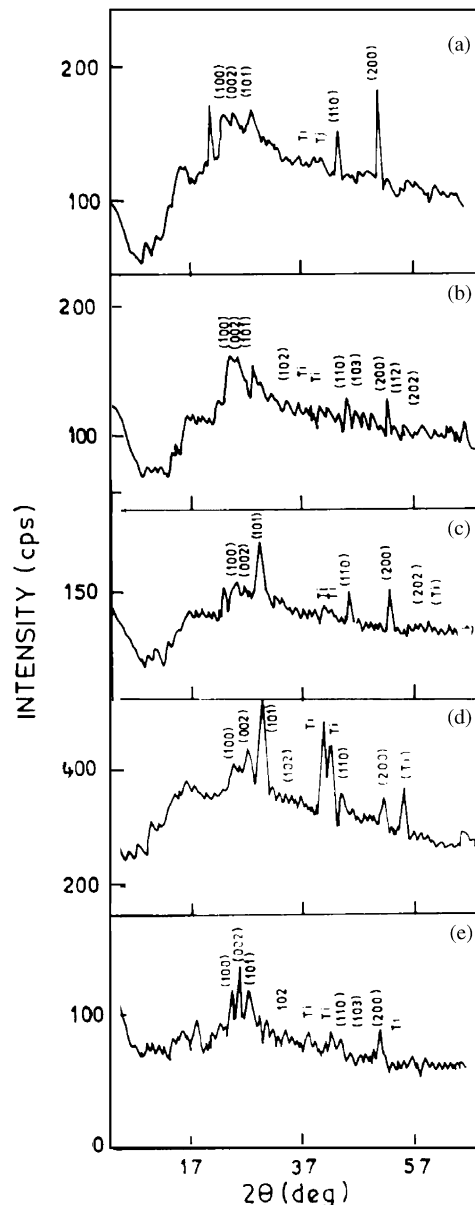


Fig. 2. XRD pattern of pulse plated $CdSeTe_{0.5}Te_{0.5}$ films at different duty cycles on a Ti substrate and annealed at 500 °C: (a) 50%, (b) 33%, (c) 15%, (d) 9% and (e) 6.25%.

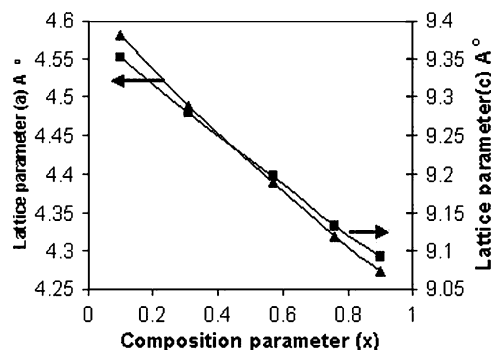


Fig. 3. Variation of lattice parameter vs. composition x .

Table 1
Lattice constants for heat-treated CdSe_xTe_{1-x} films

Composition taken	Composition observed	Duty cycle (%)	Hexagonal <i>a</i> (Å)		Hexagonal <i>c</i> (Å)	
			Standard	Observed	Standard	Observed
CdSe _{0.10} Te _{0.90}	CdSe _{0.03} Te _{0.97}	50.0	4.55	4.58	7.40	7.41
		33.3		4.58		7.41
		15.15		4.56		7.40
		9.0		4.56		7.40
		6.25		4.56		7.40
CdSe _{0.30} Te _{0.70}	CdSe _{0.28} Te _{0.72}	50.0	4.49	4.50	7.31	7.32
		33.3		4.50		7.32
		15.15		4.50		7.32
		9.0		4.50		7.32
		6.25		4.50		7.31
CdSe _{0.50} Te _{0.50}	CdSe _{0.66} Te _{0.34}	50.0	4.43	4.42	7.23	7.23
		33.3		4.42		7.23
		15.15		4.42		7.23
		9.0		4.41		7.22
		6.25		4.41		7.22
CdSe _{0.70} Te _{0.30}	CdSe _{0.79} Te _{0.21}	50.0	4.37	4.36	7.15	7.14
		33.3		4.36		7.14
		15.15		4.36		7.14
		9.0		4.36		7.13
		6.25		4.36		7.13
CdSe _{0.90} Te _{0.10}	CdSe _{0.97} Te _{0.03}	50.0	4.31	4.31	7.06	7.08
		33.3		4.31		7.08
		15.15		4.30		7.08
		9.0		4.30		7.07
		6.25		4.30		7.07

3. Results and discussion

XRD patterns of the films deposited at different duty cycles, using the precursors corresponding to 0.9 CdSe & 0.1 CdTe, show that the films are polycrystalline with cubic phase. Peaks corresponding to CdSe/Te, Cd and Ti are present, a few peaks could not be identified, and peaks corresponding to (1 1 1), (2 2 0) and (3 1 1) reflections were observed. The number of counts corresponding to (1 1 1) are found to decrease as the duty cycle decreases, this is understandable since as duty cycle decreases, the OFF time increases resulting in lower duration for the deposition time and hence a lower thickness. According to the XRD pattern of the above films after heat treatment at 500 °C for 10 min, the peak in the (1 0 0) direction was found to increase in intensity as evident from the number of counts; peaks due to Ti were observed and Cd peaks were found to disappear or decrease in intensity.

Diffraction patterns of the films 0.7 CdSe and 0.3 CdTe exhibit polycrystalline nature with cubic structure. Peaks corresponding to (1 1 1), (2 2 0), (3 1 1) and (4 0 0) of CdSe/Te along with reflections corresponding to minor peaks of Ti and Cd were also observed. As the duty cycle decreases, the (1 1 1) peak was also found to decrease. After heat treatment at 500 °C for 10 min, (1 0 0) peak was found to

increase in intensity and perfectly matched with the earlier reports.

XRD patterns of the films with equal composition of precursors CdSe and CdTe are shown in Fig. 1a–e. These films are also polycrystalline with cubic structure. The peaks corresponding to (1 1 1), (2 2 0), (3 1 1) and (4 0 0) are found; Ti peaks and Cd peaks are observed. As the duty cycle decreases, the intensity of Cd peak increases and the peak in the (1 1 1) direction decreases in intensity. After annealing (Fig 2a–e) at the same temperature as mentioned above, the peaks corresponding to CdSe/Te were observed along with the presence of Ti and absence of Cd peaks.

Films with the composition of 0.3 CdSe and 0.7 CdTe were deposited at different duty cycles and identified with XRD analysis. The films are polycrystalline with cubic structure and peaks corresponding to (1 1 1), (2 2 0), (3 1 1) and (4 0 0) and one peak corresponding to Ti are observed. As the duty cycle decreases, the peak corresponding to (1 1 1) decreases; Cd lines are also observed to appear as the duty cycle decreases. At the lowest duty cycle, several unidentified peaks are also observed.

The films deposited at different duty cycles using the precursors corresponding to 0.1 CdSe and 0.9 CdTe were traced by X-ray analysis. The films are polycrystalline with cubic structure and peaks corresponding to (1 1 1), (2 2 0),

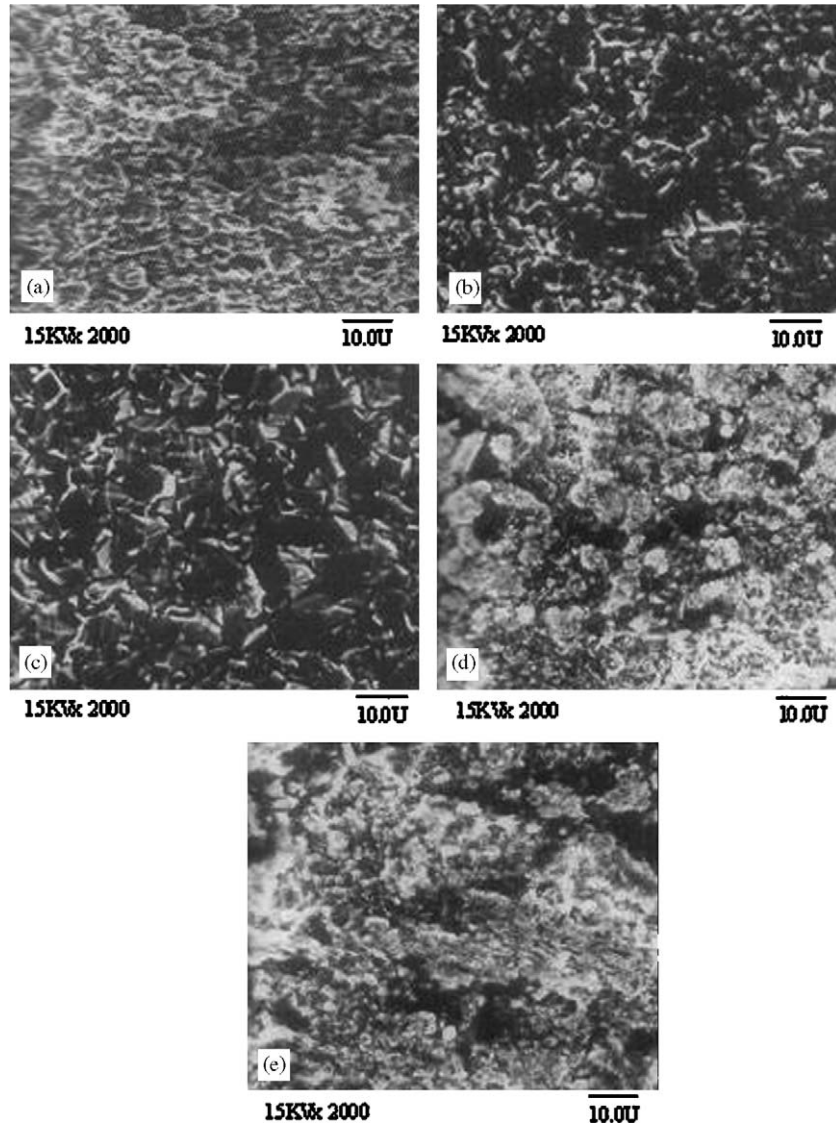


Fig. 4. SEM photograph of CdSeTe films of different compositions deposited at 9% duty cycle: (a) CdSeTe_{0.9}Te_{0.1}, (b) CdSeTe_{0.7}Te_{0.3}, (c) CdSeTe_{0.5}Te_{0.5}, (d) CdSeTe_{0.3}Te_{0.7} and (e) CdSeTe_{0.1}Te_{0.9}.

(311) and (400) were found. The peak corresponding to (400) increases up to a duty cycle of 10%; at lower duty cycles, this peak is absent.

After heat treatment, all the peaks corresponding to hexagonal phase were observed in all cases. From the XRD data of the films, the lattice parameters a and c were evaluated and they agreed well with the earlier report.

The values of lattice parameters (calculated from XRD data) with composition are shown in Fig. 3. The linear variation of the lattice parameter with composition indicates the validity of Vegard's Law [21,22]. Hence, Vegard's Law was used for the estimation of the composition

$$a_x \text{CdSe} + a_{(1-x)} \text{CdTe} = a_{\text{observed}}, \quad (1)$$

$$c_x \text{CdSe} + c_{(1-x)} \text{CdTe} = c_{\text{observed}}. \quad (2)$$

The compositions of the films are given in Table 1. In all the cases, the composition of the resulting film was different from the composition of the precursors taken. This is attributed to the fact that the deposition rates are primarily controlled by the rate of deposition of Se and Te species.

Figs. 4a–e indicate the scanning electron micrographs (SEM) of the CdSeTe films of different compositions deposited at 9% duty cycle. The micrographs indicate better crystallinity for the films rich in selenium (Fig. 4a,b); as the tellurium concentration is increased, agglomeration of particles is observed (Fig. 4c–e). These observations are in good agreement with the SEM results of CdSe and CdTe. CdSe films exhibited good crystallinity, but CdTe films exhibited agglomeration of particles.

In Fig. 5a–e, the micrographs of CdSe_{0.66}Te_{0.34} films deposited at different duty cycles and heat treated at 500 °C

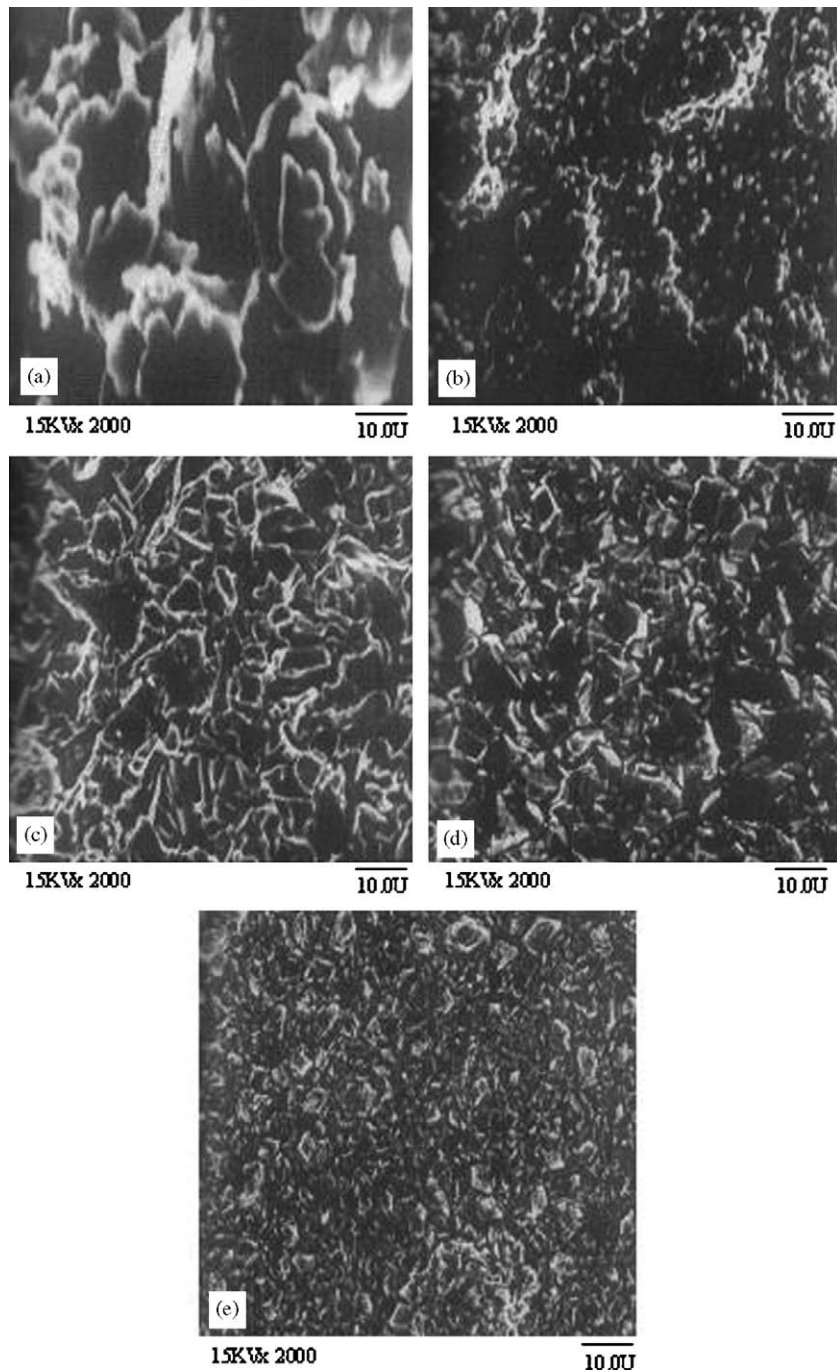


Fig. 5. SEM photograph of $\text{CdSe}_{0.5}\text{Te}_{0.5}$ films deposited at different duty cycles and heat-treated at $500\text{ }^{\circ}\text{C}$: (a) 50%, (b) 33%, (c) 15%, (d) 9% and (e) 6.25%.

are presented. As duty cycle decreases, the grain size is found to decrease; this is also reflected in the X-ray diffractograms.

Mott–Schottky plots ($1/C^2$ vs. V) were studied using 1 M Na_2SO_4 as the blocking electrolyte and an EG&G PARC impedance analyzer model 6310 (Fig. 6a–e). The $\text{CdSe}_x\text{Te}_{1-x}$ films were used as the working electrode, graphite was used as counter electrode and SCE was used as reference electrode. The frequency was fixed at 10 kHz and the bias voltage was varied in the range -1.0 to

$+0.2\text{ V}$ vs. SCE, the value of C was estimated from the imaginary part of the impedance using the relation

$$C = \frac{1}{2\pi fZ} \quad (3)$$

For all the compositions, the nature of the plot indicates n-type behavior. Extrapolation of the linear region to the voltage axis yields the flat band potential (V_{fb}) ranging from -0.8 to -1.2 V vs. SCE [12] as the composition (x) was increased in $\text{CdSe}_x\text{Te}_{1-x}$. Slope of the plot was used to

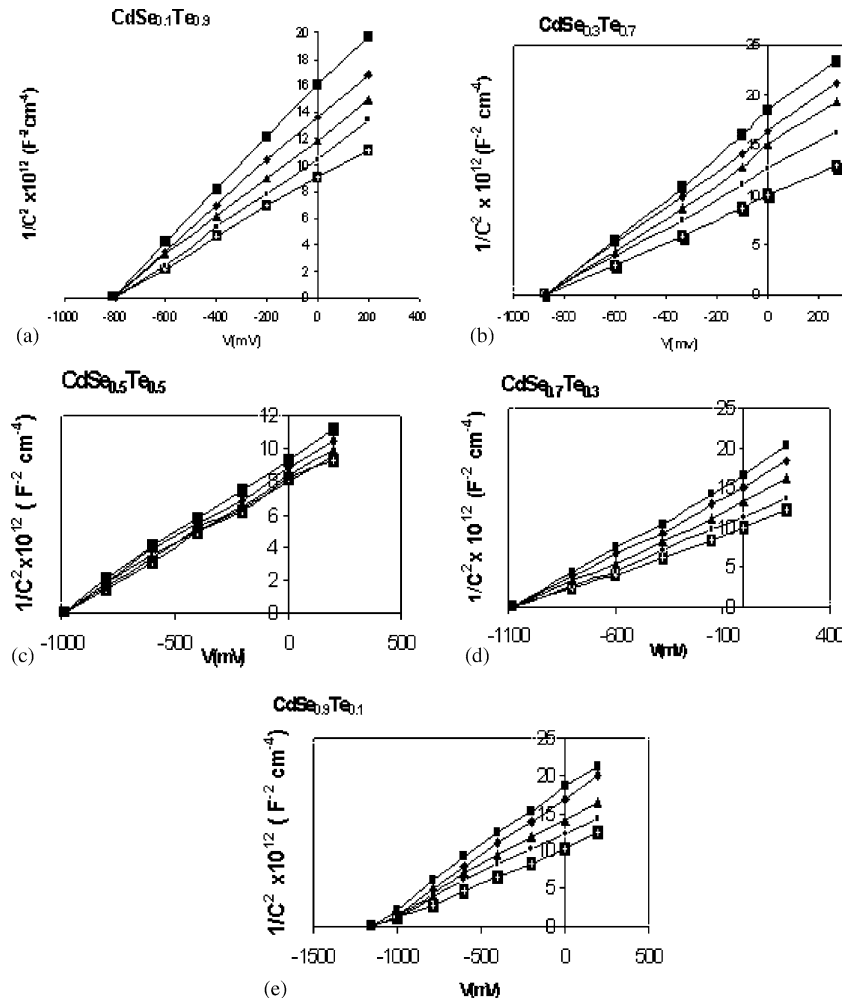


Fig. 6. Mott–Schottly plots of different compositions of CdSeTe and deposited at different duty cycles: (a) CdSeTe_{0.9}Te_{0.1}, (b) CdSeTe_{0.7}Te_{0.3}, (c) CdSeTe_{0.5}Te_{0.5}, (d) CdSeTe_{0.3}Te_{0.7} and (e) CdSeTe_{0.1}Te_{0.9}.

estimate the carrier density (N_d). The values of V_{fb} and N_d for different compositions are given in Table 2.

The conduction mechanism in semiconductors can be understood by analyzing current–voltage (I – V) plots. For single carrier injection at low voltages, the plot is generally a straight line showing the validity of Ohm’s law. However, at higher voltages, some deviation is expected. The voltage was applied using a DC power supply APLAB. The applied voltage was varied in the range 0–2.5 V. The voltage could be increased beyond 2.5 V as the films got punctured due to the lower thickness of the films. All the samples indicated linear behavior.

Semiconductor parameters like flat band potential V_{fb} , carrier concentration N_d , band bending V_b , depletion layer width W , doping density of states in conduction band N_c , conduction band E_c , Fermi level E_f of the semiconductor, valency band E_v and band gap E_g have been estimated, and the results are shown in Table 3.

The barrier height for the films deposited on different substrates is given in Table 4. From the table, it is clear that

Table 2
Variation of N_d and V_{fb} with different compositions

Compositions	$N_d \times 10^{16} \text{ cm}^{-3}$	V_{fb} (mV)
CdSe _{0.03} Te _{0.97}	0.92	–823
CdSe _{0.28} Te _{0.72}	1.21	–876
CdSe _{0.66} Te _{0.34}	4.0	–990
CdSe _{0.79} Te _{0.21}	2.81	–1080
CdSe _{0.97} Te _{0.03}	1.85	–1150

titanium possessing a work function very close to CdSe_{0.66}Te_{0.34} behaves as an ohmic contact to CdSe_{0.66}Te_{0.34}, whereas the other two contacts, nickel and stainless steel, have work functions which are not ohmic to CdSe_{0.66}Te_{0.34}, because of the difference in work function. The main shortcoming of polycrystalline photoelectrodes is recombination at grain boundaries, which is an important source of efficiency losses. This is certainly the case for

Table 3

Semiconductor parameters for CdSe_{0.66}Te_{0.34} deposited on different substrates and heat-treated at 475 °C

Semiconductor parameters	Titanium	Stainless steel	Nickel
Flat band potential V_{fb} , V_{SCE}	−0.990	−0.998	−1.06
Carrier concentration (N_d) $\times 10^{23} \text{ m}^{-3}$	4	0.98	0.01
Band bending V_b , V_{SCE}	0.40	0.46	0.48
Depletion layer width W (μm)	0.104	0.492	0.994
Doping density of states in conduction band (N_c) $\times 10^{24} \text{ m}^{-3}$	1.21	1.21	1.21
Conduction band edge E_c (eV)	−1.0092	−0.9982	−0.9562
Fermi level E_f of the semiconductor	−0.0192	−0.0372	−0.0605
Valency band edge E_v (eV)	0.5688	0.4418	0.4838
Band gap E_g (eV)	1.58	1.58	1.58

Table 4

Values of barrier height for CdSe_{0.66}Te_{0.34} films deposited at different duty cycles on nickel, stainless steel and titanium

Duty cycle	Barrier height ϕ_b (eV)		
	Stainless steel	Nickel	Titanium
50.0	0.49	0.53	Ohmic
33.3	0.49	0.55	Ohmic
15.1	0.48	0.56	Ohmic
9.9	0.48	0.57	Ohmic
6.2	0.48	0.57	Ohmic

as-electrodeposited CdSe_{0.66}Te_{0.34} films, where the grain size (d) is about two orders of magnitude lower than the light penetration depth ($1/\alpha$). Therefore, the first beneficial effect of annealing is the increase of crystallite size, so that $d > 1/\alpha$.

4. Conclusion

CdSe_{*x*}Te_{1−*x*} films exhibited a cubic structure for as-deposited films and a hexagonal structure for annealed films irrespective of the duty cycle. Composition has been calculated by using Vegard's law. Mott–Schottky plot indicated a flat band potential in the range −823 mV to −1150 mV vs. SCE, depending upon the composition. A carrier density of 10^{16} cm^{-3} was obtained. Semiconductor parameter has also been estimated.

References

- [1] M. Abramovich, M.J.P. Brasil, F. Decker, J.R. Muro, P. Motisuke, St.N. Miller, P. Salvador, J. Solid State Chem. 59 (1988) 1.
- [2] R.N. Bhattacharya, J. Appl. Electrochem. 16 (1986) 168.
- [3] M.T. Gutierrez, J. Ortega, Solar Energy Mater. 19a (1989) 383.
- [4] R. Ifflam, H.D. Banerjee, D.R. Rao, Thin Solid Films 226 (1995) 215.
- [5] V.D. Das, L. Damodhara, Solid State Commun. 99 (1995) 723.
- [6] G. Hodes, Nature 285 (1980) 110.
- [7] G. Hodes, D. Cahen, J. Manassen, M. David, J. Electro-chem. Soc. 127 (1980) 2252.
- [8] L.D. Udayaunaya, A.M. Pavellets, L.W. Khanat, V.E. Badam, Thin Solid Films 138 (1986) 113.
- [9] P.J. Sebastian, V. Sivaramakrishnan, J. Phys. D. Appl. Phys. 23 (1990) 1114.
- [10] Z. Loizos, N. Spyrellis, G. Maurin, Surf. Coat. Technol. 45 (1991) 273.
- [11] S. Uthanna, P.J. Reddy, Solid State Commun. 45 (1983) 979.
- [12] V. Swaminathan, K.R. Murali, J. Appl. Electrochem. 32 (2002) 1151.
- [13] JCl. Puipe, N. Ibl, J. Appl. Electrochem. 10 (1980) 725.
- [14] V. Swaminathan, K.R. Murali, Acta Mater., for communication.
- [15] K.R. Murali, V. Subramanian, N. Rengarajan, K.N. Rao, A.S. Lakshmanan, Bull. Electrochem. 6 (1990) 437.
- [16] N.F. Mott, Proc. R. Soc. A 171 (1939) 27.
- [17] W. Schottky, Z. Phys. 113 (1939) 367.
- [18] H. Gerisher, Adv. Electrochem. Eng. 1 (1961) 139.
- [19] J.A. Wilson, A.D. Yoffew, Adv. Phys. 18 (1969) 193.
- [20] S. Chandra, D.P. Singh, P.C. Srivastava, S.N. Sahu, J. Phys. D. Appl. Phys. 17 (1984) 1261.
- [21] H.P. Klung, L.E. Alexander, X-ray Diffraction Procedures, 1954; G.L. Clark, Applied X-rays, McGraw-Hill, New York, 1955.